

Graviton mass reduces tension between early and late time cosmological data

Antonio De Felice

Center for Gravitational Physics, Yukawa Institute for Theoretical Physics, Kyoto University, 606-8502, Kyoto, Japan

Shinji Mukohyama

Center for Gravitational Physics, Yukawa Institute for Theoretical Physics, Kyoto University, 606-8502, Kyoto, Japan and

Kavli Institute for the Physics and Mathematics of the Universe (WPI),

UTIAS, The University of Tokyo, 277-8583, Chiba, Japan

(Dated: December 9, 2024)

The standard Λ -CDM predicts a growth of structures which tends to be higher than the values of redshift space distortion measurements, if the cosmological parameters are fixed by the CMB data. In this paper we point out that this discrepancy can be resolved/understood if we assume that the graviton has a small but non-zero mass. In the context of the Minimal Theory of Massive Gravity (MTMG), due to infrared Lorentz violations measurable only at present cosmological scales, the graviton acquires a mass without being haunted by unwanted extra degrees of freedom. It is possible to choose a branch of cosmological solutions in MTMG for which the background is the same as that in GR but the evolution of matter perturbations gets modified by the graviton mass. On studying the fit of such modified dynamics to the above-mentioned redshift distortion measurements, we find that the Λ -CDM model is less probable than MTMG by three orders of magnitude. The data also pin-down the graviton mass around $\mu \approx 9.8 \times 10^{-33}$ eV, which is consistent with the latest upper bound $\mu < 1.2 \times 10^{-22}$ eV set by the recent LIGO observation.

Most recent low-redshift (i.e. late-times) cosmological data [1–16] describing the growth of structures tend to be in tension with respect to high-redshift (i.e. early-times) CMB data. The Λ -CDM in General Relativity (GR) is in excellent agreement with data from CMB experiments such as Planck [17]. Nonetheless, once the cosmological parameters are fixed by the CMB data, GR predicts a growth of structures which tends to be higher than the values of redshift space distortion measurements. When the perihelion shift of Mercury was found in the 19th Century, people tried to explain it by introducing an unknown planet called “Vulcan,” so to speak a dark planet. The right answer, however, was not a dark planet but to change gravity, from Newton’s theory to GR. One might thus ask whether the tension between early and late time cosmological data can be relaxed by modifying gravity at long distances. In GR, because of gravity’s attractive nature, adding dynamical dark energy usually enhances the growth of structures and thus does not seem to help. In fact, history might actually repeat itself. Masses and spins are the most fundamental properties of particles and fields. For this reason, one of the most interesting possibilities for modification of gravity is to give a mass to the graviton, a spin-2 particle mediating gravity. The purpose of the present paper is to point out that the discrepancy between early and late time cosmological data can be resolved/understood if we assume that the graviton has a small but non-zero mass.

While a nonlinear theory of massive gravity stable around a Minkowski background, called the dRGT theory, was discovered in 2010 [20], it was later shown that all homogeneous and isotropic cosmological solutions in the theory are unstable [21]. The MTMG [18] has then been introduced in order to get rid of the un-

wanted, unstable degrees of freedom. By explicitly breaking Lorentz invariance at cosmological scales, constraints were imposed to the system as to leave only the tensor modes to propagate, as in GR. There are two distinct branches of cosmological solutions in MTMG: one branch that provides a stable nonlinear completion of the self-accelerating solution [22] in dRGT theory and the other branch that we shall consider in the present paper. In the latter branch, often called the normal branch, of MTMG, it is possible to choose the fiducial metric so that the cosmological background behaves exactly as the Λ -CDM. Therefore, on the background, MTMG is described by one single free parameter ρ_Λ stemming from the graviton mass¹, as

$$3H^2 = 8\pi G_N (\rho_m + \rho_\Lambda), \quad (H^2)' = -8\pi G_N (\rho_m + P_m). \quad (1)$$

where H is the Hubble expansion rate, G_N is Newton’s constant, ρ_m and P_m are energy density and pressure of matter, and a prime denotes derivative with respect to the e-fold time-variable: $\mathcal{N} = -\ln(1+z)$, and z is the cosmological redshift. Furthermore, on studying the influence of the theory on the matter sector, it was found that in cosmological linear perturbation theory, the evolution of each mode differs from the Λ -CDM only for low redshifts [23]. In fact, the dynamics of dust perturbations

¹ In terms of the constant ratio X_0 of the scale factor of the fiducial metric to that of the physical metric, and the free parameters m and c_i ($i = 1, \dots, 4$) of MTMG, we have $\rho_\Lambda \equiv \frac{m^2}{16\pi G_N} (c_1 X_0^3 + 3c_2 X_0^2 + 3c_3 X_0 + c_4)$.

($P_m = 0$) is described by

$$\delta_m'' + \left(2 - \frac{3}{2}\Omega_m\right)\delta_m' + \left(\frac{9\theta Y\Omega_m}{2(\theta Y - 2)^2} + \frac{3}{\theta Y - 2}\right)\Omega_m\delta_m = 0, \quad (2)$$

where δ_m is the matter perturbation, $\Omega_m = \frac{8\pi G_N \rho_m}{3H^2}$, $Y \equiv \frac{H_0^2}{H^2}$, $\theta \equiv \frac{\mu^2}{H_0^2}$, $H_0 = H(\mathcal{N} = 0)$, and μ is the mass of the gravitational waves². Therefore, at the level of perturbations, we find the second free parameter, θ . In order for the tensor modes to be stable, we require that $\theta \geq 0$. In the limit $\theta \rightarrow 0$, we recover the evolution equation for the perturbations in the Λ -CDM. This same limit is achieved by $Y \rightarrow 0$, i.e. at early times. The evolution equations for Ω_m and Y read as follows

$$\Omega_m' = 3\Omega_m(\Omega_m - 1), \quad Y' = 3Y\Omega_m. \quad (3)$$

Furthermore we impose the system to satisfy the following boundary conditions at a point of high redshift, e.g. $\mathcal{N} = \mathcal{N}_i = -6$ corresponding to $z = z_i \simeq 402.4$, and at the present time, $\mathcal{N} = 0$: $\delta_m'(\mathcal{N}_i) = \delta_m(\mathcal{N}_i)$ (selecting the growing mode at early times), $Y(\mathcal{N} = 0) = 1$ (by definition), and $\Omega_m(\mathcal{N} = 0) = 0.3089$ (fixing, once for all, the only background parameter ρ_Λ to the Λ -CDM best-fit value[17]). One may set $\delta_m(\mathcal{N}_i)$ to any non-zero value since the overall amplitude of δ_m does not affect the observable defined below.

The observable we will use to constrain the only remaining free parameter, θ , is defined as $y(z) \equiv f(z)\sigma_8(z)$, where $f(z) = \delta_m'/\delta_m$, and $\sigma_8(z)$ is the rms mass fluctuation of a sphere of radius 8 Mpc. Assuming a window function which is only dependent on k and on the radius of the spherical distribution of mass, we find that $\sigma_8(z) \propto \delta_m(z)$. We can thus write $\sigma_8(z) = \sigma_8(z_i)\delta_m(\mathcal{N})/\delta_m(\mathcal{N}_i)$. Since GR and MTMG are indistinguishable at early times and their backgrounds are exactly the same for all times, the CMB data give the same constraint on the value(s) of $\sigma_8(z_i)$ (and $\Omega_m(\mathcal{N} = 0)$) for both theories. In GR we know that its best fit is given by $\sigma_8^{\text{GR}}(z = 0) = 0.8159$ and we can determine $\sigma_8(z_i)$ (common for GR and MTMG) by using the evolution for δ_m^{GR} , so that $\sigma_8(z_i) = 0.8159\delta_m^{\text{GR}}(\mathcal{N}_i)/\delta_m^{\text{GR}}(0)$. Having defined the observable, $y(z)$, we can now introduce the chi-square functions as follows

$$\chi_{\text{MTMG}}^2 \equiv \sum_n \frac{(y_n - y_n^{\text{MTMG}})^2}{\sigma_n^2}, \quad \chi_{\text{GR}}^2 \equiv \sum_n \frac{(y_n - y_n^{\text{GR}})^2}{\sigma_n^2}, \quad (4)$$

where the index n runs over the data points reported in Table 1, y_n and σ_n are the observed value of y and its uncertainty for the n -th data point, and y_n^{MTMG}

TABLE I. Data points

z	$f\sigma_8$	Refs.
0.02	0.360 ± 0.04	[1]
0.067	0.423 ± 0.055	[2]
0.15	0.490 ± 0.15	[3]
0.17	0.510 ± 0.06	[4, 5]
0.22	0.420 ± 0.07	[6]
0.25	0.351 ± 0.058	[7]
0.3	0.408 ± 0.0552	[8]
0.32	0.394 ± 0.062	[9]
0.35	0.440 ± 0.05	[5, 10]
0.37	0.460 ± 0.038	[7]
0.4	0.419 ± 0.041	[8]
0.41	0.450 ± 0.04	[6]
0.44	0.413 ± 0.08	[11]
0.5	0.427 ± 0.043	[8]
0.57	0.444 ± 0.038	[9]
0.59	0.488 ± 0.06	[12]
0.6	0.430 ± 0.04	[6]
0.6	0.390 ± 0.063	[13]
0.73	0.437 ± 0.072	[13]
0.77	0.490 ± 0.18	[5, 14]
0.78	0.380 ± 0.04	[6]
0.8	0.470 ± 0.08	[15]
1.36	0.482 ± 0.116	[16]

and y_n^{GR} are the corresponding theoretical predictions in MTMG and GR, respectively. Notice that χ_{GR}^2 is not a function of any parameter, but merely a number. On the other hand, χ_{MTMG}^2 is a function only of the parameter θ (all the initial conditions are completely fixed). On using the data points reported in Table 1, we plot $\chi_{\text{MTMG}}^2(\theta)$ in Fig. 1. It should be noticed that $\chi_{\text{MTMG}}^2(\theta)$ has a minimum at $\theta_{\min} \approx 1.165$ and then rapidly increases for larger values of θ . On defining the likelihood function as $\mathcal{L} = \exp[-\chi_{\text{MTMG}}^2/2]$, and sampling it via the MCMC method³, we obtain, in Fig. 2, a likelihood plot for the free parameter θ , leading to $\theta = 1.165^{+0.070}_{-0.176}$ at 68.27% C.L.⁴ Besides, we numerically find that, for MTMG, $\chi_{\text{MTMG}}^2(\theta)$ possesses a minimum as $\chi_{\text{MTMG}}^2(\theta_{\min} \approx 1.165) \equiv \bar{\chi}_{\text{MTMG}}^2 \approx 10.876$ whereas, for GR, we have $\chi_{\text{GR}}^2 = \chi_{\text{MTMG}}^2(\theta = 0) \approx 24.51$.

Following the Akaike Information Criterion (AIC) [25], used to compare the relative likelihood of two models, we find that in this case GR is $\exp[(\bar{\chi}_{\text{MTMG}}^2 + 2 - \chi_{\text{GR}}^2)/2] \approx 3 \times 10^{-3}$ as probable as MTMG. This result is already interesting in terms of model building, as it states that

² In MTMG, we have $\mu^2 = \frac{1}{2}X_0(c_1X_0^2 + 2c_2X_0 + c_3)m^2$ (see footnote 1 as well).

³ For this aim, we have made use of the **emcee** package [24].

⁴ We find that, for the best-fit of MTMG, $\sigma_8(0) \approx 0.785$.

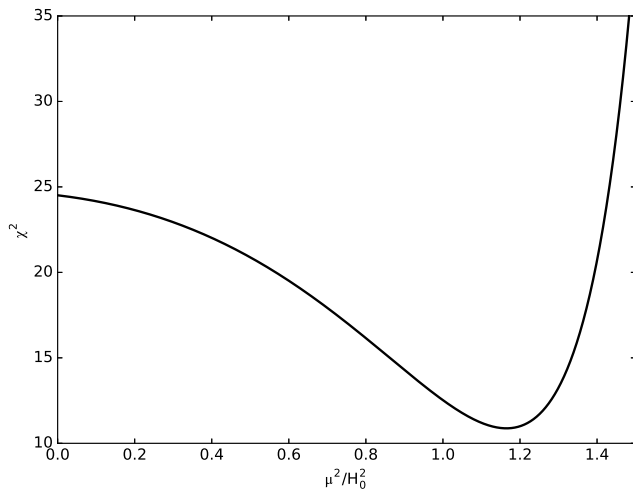


FIG. 1. The chi-square for MTMG, χ_{MTMG}^2 , as a function of the parameter $\theta = \mu^2/H_0^2$. GR is recovered for $\theta = 0$.

the data lead to a larger likelihood for MTMG compared to Λ -CDM. Moreover, from the theoretical point of view, the redshift-space-distortion measurements do set the value of the graviton mass squared to be $\mu^2 = \theta H_0^2 = 1.165^{+0.070}_{-0.176} H_0^2$. This is consistent with the upper bound on the graviton mass set by the LIGO collaboration [19].

Finally, in Fig. 3, we plot the data and the GR fit (red dashed line) together with the best MTMG fit (thick black line), whereas in Fig. 4 we show the evolution of the effective gravitational constant for the perturbations⁵, G_{eff}/G_N , as a function of redshift and of $1/Y = \rho_{\text{tot}}/\rho_{\text{tot},0}$, where $\rho_{\text{tot}} = \rho_m + \rho_\Lambda$ is the total energy density and $\rho_{\text{tot},0}$ is its present value. Fig. 4 shows deviation of MTMG from GR, $|G_{\text{eff}}/G_N - 1| > 0.01$, only for $z < 3.53$, which translates to $\rho_{\text{tot}} < 30\rho_{\text{tot},0}$. This observation, combined with the fact that in MTMG there is no scalar/vector degree of freedom to screen [18], indicates that we will recover GR when the matter density of the environment, ρ_{env} , is much higher than $\rho_{\text{tot},0}$. For example, inside the galaxy and the solar system, ρ_{env} is high enough to suppress any deviations from GR. On the other hand, as for the growth of large scale structures at low redshift, corresponding to low ρ_{env} , Figs. 3 and 4 clearly show deviations of MTMG from GR, which greatly help reconciling the redshift-space distortion data to the CMB data.

In summary, in the context of MTMG a small but non-zero graviton mass tends to reduce the tension between early-time and late-time data sets. It also provides a model for the evolution of matter perturbations

⁵ In MTMG, it is read off from the coefficient of the last term in (2) as $\frac{G_{\text{eff}}}{G_N} = -\frac{2}{3} \left(\frac{9\theta Y \Omega_m}{2(\theta Y - 2)^2} + \frac{3}{\theta Y - 2} \right)$.

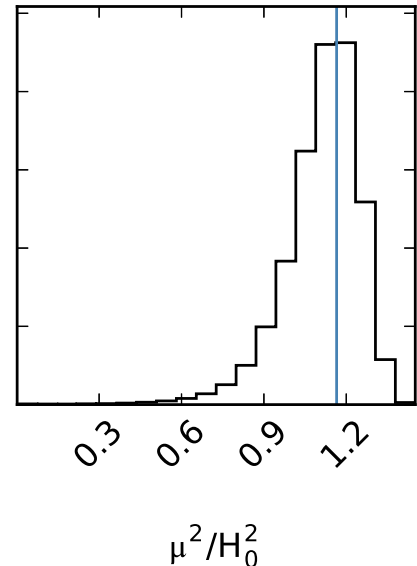


FIG. 2. Distribution of the parameter $\theta = \mu^2/H_0^2$ according to the likelihood function defined via the χ_{MTMG}^2 . We have given flat prior to the parameter θ , in the range $0 \leq \theta < 1.9$. Negative values for θ give a negative mass squared for the graviton, whereas larger values for θ lead Y to reach the point $Y_\infty = 2/\theta$, at which G_{eff} switches sign and the last term in (2) diverges. The blue line indicates the value of the maximum likelihood point, i.e. the minimum of χ_{MTMG}^2 .

which can be further studied for the implications that the existence of a non-zero-mass graviton might have. This model can be further tested against future experiments/measurements related to the cosmological-scale dynamics of the CDM dust fluid.

ADF was supported by JSPS KAKENHI Grant Numbers 16K05348, 16H01099. SM was supported in part by JSPS KAKENHI Grant Number 24540256 and World Premier International Research Center Initiative (WPI), MEXT, Japan.

-
- [1] M. J. Hudson and S. J. Turnbull, *Astrophys. J. Let.* **715**, 30 (2012).
 - [2] F. Beutler, et al., *Mon. Not. Roy. Astron. Soc.*, **423**, 3430 (2012).
 - [3] C. Howlett, A. Ross, L. Samushia, W. Percival and M. Manera, *Mon. Not. Roy. Astron. Soc.* **449**, no. 1, 848 (2015).
 - [4] W. J. Percival, et al., *Mon. Not. Roy. Astron. Soc.*, **353**, 1201 (2004).
 - [5] Y.-S. Song and W.J. Percival, *J. Cosmol. Astropart. Phys.*, **10** (2009) 004.
 - [6] C. Blake et al., *Mon. Not. Roy. Astron. Soc.*, **415**, 2876

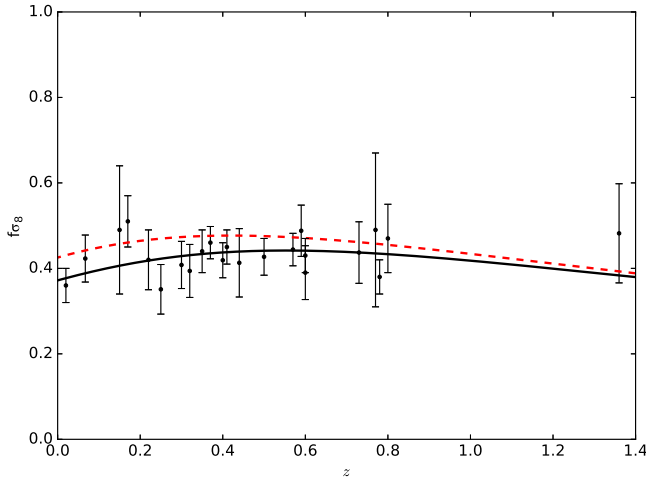


FIG. 3. Fit to the data for GR (red dashed line), and MTMG (thick black line).

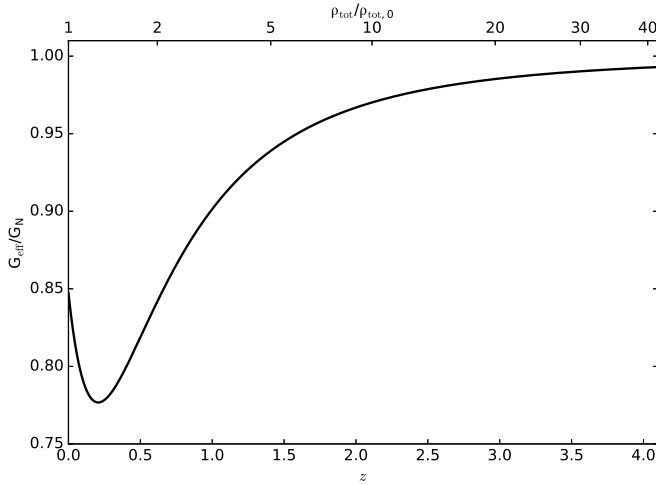


FIG. 4. Evolution of G_{eff}/G_N as a function of redshift (lower x -axis), and of $\rho_{\text{tot}}/\rho_{\text{tot},0}$ (upper x -axis), for the best fit of MTMG.

- (2011).
- [7] L. Samushia, W. J. Percival and A. Raccanelli, Mon. Not. Roy. Astron. Soc., **420**, 2102 (2012).
 - [8] R. Tojeiro et al., Mon. Not. R. Astron. Soc., **424**, 2339 (2012).
 - [9] H. Gil-Marín, et al., Mon. Not. R. Astron. Soc., 10.1093/mnras/stw1096 (2016).
 - [10] M. Tegmark et al., Phys. Rev. D **74**, 123507 (2006).
 - [11] C. Blake et al., Mon. Not. R. Astron. Soc., **425**, 405 (2012).
 - [12] C. H. Chuang *et al.*, arXiv:1312.4889.
 - [13] E. Macaulay, I. K. Wehus and H. K. Eriksen, Phys. Rev. Lett. **111**, no. 16, 161301 (2013).
 - [14] L. Guzzo et al., Nature **451**, 541 (2008).
 - [15] S. de la Torre *et al.*, Astron. Astrophys. **557**, A54 (2013).
 - [16] T. Okumura *et al.*, Publ. Astron. Soc. Jap. **68**, 47 (2016).
 - [17] P. A. R. Ade *et al.* [Planck Collaboration], arXiv:1502.01589 [astro-ph.CO].
 - [18] A. De Felice and S. Mukohyama, Phys. Lett. B **752**, 302 (2016).
 - [19] B. P. Abbott *et al.* [LIGO Scientific and Virgo Collaborations], Phys. Rev. Lett. **116**, no. 6, 061102 (2016); Phys. Rev. Lett. **116**, no. 22, 221101 (2016).
 - [20] C. de Rham and G. Gabadadze, Phys. Rev. D **82**, 044020 (2010); C. de Rham, G. Gabadadze and A. J. Tolley, Phys. Rev. Lett. **106**, 231101 (2011).
 - [21] A. De Felice, A. E. Gumrukcuoglu and S. Mukohyama, Phys. Rev. Lett. **109**, 171101 (2012).
 - [22] A. E. Gumrukcuoglu, C. Lin and S. Mukohyama, JCAP **1111**, 030 (2011); JCAP **1203**, 006 (2012).
 - [23] A. De Felice and S. Mukohyama, JCAP **1604**, no. 04, 028 (2016).
 - [24] D. Foreman-Mackey, D. W. Hogg, D. Lang and J. Goodman, Publ. Astron. Soc. Pac. **125**, 306 (2013); J. Goodman and J. Weare, Comm. App. Math. Comp. Sci., 5(1), 65 (2010).
 - [25] H. Akaike, IEEE Trans. Automatic Control **19**, 716 (1974); N. Sugiura, Commun. Stat. **A7**, 13 (1978).